RUNNING TITLE: OC oxidation processes across vegetation

Carbon inputs from riparian vegetation limit oxidation of physically-bound organic carbon via biochemical and thermodynamic processes

Emily B. Graham[1], Malak M. Tfaily[2], Alex R. Crump[1], Amy E. Goldman[1], Evan Arntzen[1], Elvira Romero[1], C. Tom Resch[1], David W. Kennedy[1], and James C. Stegen[1]

[1]Pacific Northwest National Laboratory, Richland, WA USA

[2]Environmental Molecular Science Laboratory, Richland, WA USA

Correspondence: Emily B. Graham, Pacific Northwest National Laboratory, PO Box 999, Richland, WA 99352, 509-372-6049, emily.graham@pnnl.gov

Keywords: terrestrial-aquatic interface, priming, recalcitrant, labile, FT-ICR-MS, aerobic metabolism, hyporheic zone

Key points.

- Riparian vegetation protects bound-OC stocks
- Biochemical and metabolic OC oxidation processes vary with vegetation
- Common thermodynamic principles underlie OC oxidation regardless of vegetation

Abstract.

In light of increasing terrestrial carbon (C) transport across aquatic boundaries, the mechanisms governing organic carbon (OC) oxidation along terrestrial-aquatic interfaces are crucial to future climate predictions. Here, we investigate the biochemistry, metabolic pathways, and thermodynamics corresponding to OC oxidation in the Columbia River corridor using ultra-high resolution C characterization. We leverage natural vegetative differences to encompass variation in terrestrial C inputs. Our results suggest that decreases in terrestrial C deposition associated with diminished riparian vegetation induce oxidation of physically-bound OC. We also find that contrasting metabolic pathways oxidize OC in the presence and absence of vegetation and—in direct conflict with the 'priming' concept—that inputs of water-soluble and thermodynamically favorable terrestrial OC protects bound-OC from oxidation. In both environments, the most thermodynamically favorable compounds appear to be preferentially oxidized regardless of which OC pool microbiomes metabolize. In turn, we suggest that the extent of riparian vegetation causes sediment microbiomes to locally adapt to oxidize a particular pool of OC, but that common thermodynamic principles govern the oxidation of each pool (e.g., water-soluble or physically-bound). Finally, we propose a mechanistic conceptualization of OC oxidation along terrestrial-aquatic interfaces that can be used to model heterogeneous patterns of OC loss under changing land cover distributions.

1. Introduction

Soils and nearshore sediments comprise a carbon (C) reservoir that is 3.2 times larger than the atmospheric C pool [*Burd et al.*, 2016], yet Earth System Models (ESMs) struggle to integrate mechanisms of OC oxidation in these environments into predictions of atmospheric carbon dioxide concentrations [*Todd-Brown et al.*, 2013; *Wieder et al.*, 2013; *Wieder et al.*, 2015]. In particular, OC oxidation in nearshore habitats constitutes a significant uncertainty in atmospheric C flux [*Aalto et al.*, 2003; *Battin et al.*, 2009] and knowledge on C cycling along these transitional ecosystems is necessary to accurately predict global C cycling [*Burd et al.*, 2016]. Terrestrial C inputs into aquatic systems have nearly doubled since pre-industrial times; an estimated 2.9 Pg C now crosses terrestrial-aquatic interfaces annually (vs. 0.9 Pg C yr^{-1} stored within forested ecosystems) [*Battin et al.*, 2008; *Regnier et al.*, 2013]. The magnitude of this flux has garnered significant recent attention [*Battin et al.*, 2008; *Battin et al.*, 2009; *Regnier et al.*, 2013], yet the biochemical, metabolic, and thermodynamic mechanisms governing OC oxidation along aquatic interfaces remain a crucial uncertainty in climate predictions. New molecular techniques are providing insight into OC dynamics [*Mason et al.*, 2016; *Malak M Tfaily et al.*, 2015; *M.M. Tfaily et al.*, 2017], but we still lack an understanding of why some OC remains stabilized for millennia whereas other OC is rapidly oxidized [*Schmidt et al.*, 2011].

The ability of microorganisms to oxidize complex OC is an important constraint on C cycling, as OC is a mixture of compounds with different propensities for biotic oxidation [*J Hedges and Oades*, 1997; *J I Hedges et al.*, 2000]. Within terrestrial research, OC oxidation is often framed within the concept of 'priming', whereby microbial oxidation of chemically-complex, less bioavailable OC is fueled by the addition of more bioavailable and thermodynamically favorable OC compounds [*Kuzyakov*, 2010]. However, the applicability of

45 priming in aquatic environments is unclear [*Bengtsson et al.*, 2014; *Bianchi*, 2011; *Guenet et al.*,
46 2010]. Aquatic systems, and in particular nearshore environments, frequently experience mixing
47 of terrestrial and aquatic C sources with distinct chemical character, providing a theoretical basis
48 for priming expectations [*Bengtsson et al.*, 2014; *Guenet et al.*, 2010]. Consistent with priming,
49 *Guenet et al.* [2010] have proposed that this mixing generates "hotspots" or "hot moments" of
50 biological activity facilitated by complementary C resources. Alternatively, OC stabilization in
51 sediments is tightly linked to organomineral interactions, which provide physical protection from
52 extracellular enzyme activity [*J I Hedges and Keil*, 1995; *Hunter et al.*, 2016; *Rothman and*
53 *Forney*, 2007], and the strength of these interactions may override any influence of priming.
54 Early investigations of priming effects in aquatic systems have been inconclusive, with evidence
55 both for [*Dorado-García et al.*, 2016] and against [*Bengtsson et al.*, 2014; *Catalán et al.*, 2015]
56 priming mechanisms.

57 Several new perspectives have attempted to move beyond frameworks, such as priming,
58 that depend on strict chemical definitions to predict OC oxidation [*Burd et al.*, 2016; *Cotrufo et*
59 *al.*, 2013; *Lehmann and Kleber*, 2015]. Recent work proposes that the probability of OC
60 oxidation is related to a spectrum of chemical properties and that even very complex OC can be
61 oxidized when more thermodynamically favorable OC is depleted or isolated from
62 microorganisms. For example, *Lehmann and Kleber* [2015] have proposed a 'soil continuum
63 hypothesis' whereby OC is a gradient of continuingly decomposing compounds that are variably
64 accessible for biotic oxidation, with no notion of chemically labile versus recalcitrant
65 compounds. Similarly, *Burd et al.* [2016] have suggested that OC oxidation is a 'logistical
66 problem' involving the ability of microorganisms to access and metabolize compounds. Both

concepts capture the emerging belief that chemically-complex, less thermodynamically favorable OC can be oxidized when more favorable compounds are inaccessible.

Here, we address a critical knowledge gap in predicting the global C balance [*Aalto et al.*, 2003; *Battin et al.*, 2009; *Burd et al.*, 2016; *Regnier et al.*, 2013]—mechanisms governing OC oxidation along terrestrial-aquatic interfaces. Specifically, we investigate the biochemistry, microbial metabolism, and thermodynamics of OC oxidation in nearshore water-soluble and physically-bound (i.e., mineral and microbial) OC pools along a freshwater terrestrial-aquatic interface. We leverage natural variation in riparian vegetation along the Columbia River in Eastern Washington State, the largest river in the U.S. west of the Continental Divide [*Ebel et al.*, 1989; *Moser et al.*, 2003], to examine these mechanisms in the context of spatial variation in terrestrial C deposition. Consistent with the priming paradigm, we hypothesize that (a) C deposition associated with riparian vegetation increases total aerobic metabolism and enhances oxidation of bound-OC stocks, while (b) areas without riparian vegetation foster lower rates of aerobic metabolism with minimal oxidation of bound-OC.

2. Materials and Methods

2.1. Site Description

This study was conducted along the Columbia River shoreline within the Hanford 300 Area (approximately 46^{o} 22’ 15.80”N, 119^{o} 16’ 31.52”W) in eastern Washington State [*Graham et al.*, 2016a; 2017; *Slater et al.*, 2010; *Zachara et al.*, 2013]. The Columbia River experiences shoreline geographic variation in vegetation patterns, substrate geochemistry, and microbiome composition [*Arntzen et al.*, 2006; *Lin et al.*, 2012; *Peterson and Connelly*, 2004; *Slater et al.*, 2010; *Stegen et al.*, 2016; *Stegen et al.*, 2012; *Zachara et al.*, 2013]. Accordingly, the Hanford

Reach of the Columbia River embodies an ideal natural system in which to examine heterogeneity of terrestrial OC inputs and subsequent OC oxidation mechanisms.

Liquid N_2-frozen sediment profiles (0-60 cm) were collected along two shoreline transects with or without riparian vegetation (hereafter, V and NV for 'vegetated' and 'not vegetated', Table 1) perpendicular to the Columbia River in March 2015, separated by a distance of ~170m. V was characterized by a moderately sloping scour zone, small boulders, and a closed canopy of woody perennials *Morus rubra* (Red Mulberry) and *Ulmus rubra* (Slippery Elm). Upper bank samples were collected within the root zone. In contrast, NV was characterized by a gradually sloping scour zone, cobbled armor layer, and no vegetation. We collected profiles at three locations in each transect with 5m spacing within a spatial domain of ~175 x 10m. In each transect, the lower bank profile was located at ~0.5m (vertical distance) below the water line and the upper bank profile was located ~0.5m (vertical distance) above the water line (approximately 10m horizontal distance), with the third profile situated at the midpoint. Each profile was sectioned into 10-cm intervals from 0-60cm. Because OC composition (see below for Methods) did not differ across upper (0-10cm) to lower (50-60cm) sections in each profile, each 10-cm section was used as a replicate sample to provide sufficient sample size (n >15 at each transect) for cross-site comparisons.

2.2. Sample Collection

Liquid N_2-frozen sediment profiles were collected as outlined in *Moser et al.* [2003] using a method developed by *Lotspeich and Reed* [1980] and modified by *Rood and Church* [1994]. A pointed stainless steel tube (152 cm length, 3.3 cm outside diameter, 2.4 cm inside diameter) was driven into the river bed to a depth of ~60cm. Liquid N_2 was poured down the

tube for ~15 minutes, until a sufficient quantity of material had frozen to the outside of the rod. The rod and attached material were removed from the riverbed with a chain hoist suspended beneath a tripod. Profiles were placed over an aluminum foil lined cooler containing dry ice. Frozen material was removed with a mallet. The material was then wrapped in the foil and transported on dry ice to storage at -80°C. In the lab, profiles were sectioned into 10cm depth intervals from 0-60 cm (n = 6 per profile, except for NV3 which was sectioned only from 30-60cm; total n = 33)

2.3. Physicochemistry

Details concerning physicochemical assays are provided in the Supporting Information. Briefly, we determined the particle distribution of sediments by separating size fractions via sieving; total nitrogen, sulfur, and carbon content were determined using an Elementar vario EL cube (Elementar Co.Germany); NH_4^+ was extracted with KCl and measured with Hach Kit 2604545 (Hach, Loveland, Co); iron content was measured with a ferrozine assay; and all other ion concentrations were measured by inductively coupled plasma mass spectrometry (ICP-MS) on HCl extractions. Aerobic metabolism was determined with a resazurin reduction assay, modified from *Haggerty et al.* [2009].

2.4. FT-ICR-MS solvent extraction and data acquisition

We leverage state of science chemical extraction protocols combined with Electrospray ionization (ESI) and Fourier transform ion cyclotron resonance (FT-ICR) mass spectrometry (MS) to infer differences in OC character among our samples. Previously, *Tfaily et al.* [2015; 2017] have demonstrated the optimization of OC characterization from soils and sediments by

sequential extraction with polar and non-polar solvents tailored to the sample set of interest. Tfaily's extraction procedures have been coupled to ESI FT-ICR-MS to distinguish OC pools among ecosystems and soil types [*Tfaily et al.*, 2015; *Tfaily et al.*, 2017] as well as to provide information on the metabolism of distinct OC pools among samples within a single environment [*Bailey et al.*, 2017]. Other common OC characterization methods such as nuclear magnetic resonance spectroscopy (NMR), Fourier transform infrared spectroscopy (FT-IR), and gas chromatography MS only analyze a limited number of compound classes [*Kögel-Knabner*, 2002; *Kögel-Knabner*, 2000]. In contrast, ESI FT-ICR-MS introduces intact organic molecules into the MS without fragmentation and allows for the detection of a wide range of chemical compounds [*Tfaily et al.*, 2015; *Tfaily et al.*, 2017]. The use of 12 Tesla (T) FT-ICR-MS offers high mass resolving power (>1M) and mass measurement accuracy (<1 ppm), and while nascent in its application within complex environmental systems, it has emerged as a robust method for determining OC chemistry of natural organic matter [*Kim et al.*, 2003; *Koch et al.*, 2005; *Tfaily et al.*, 2011; *Tremblay et al.*, 2007]. Moreover, *Tfaily et al.* [2015; 2017] have demonstrated that sequential extraction with targeted solvents can preferentially select OC pools with differing chemical character (e.g., lipid-like vs. carbohydrate-like).

Here, we used three solvents with different polarities —water (H_2O), methanol (CH_3OH, hereafter "MeOH") and chloroform ($CHCl_3$)—to sequentially extract a large diversity of organic compounds from samples, according to *Tfaily et al.* [2015; 2017]. Water extractions were performed first, followed by MeOH and then $CHCl_3$. Previous work has shown that each solvent is selective towards specific types of compounds [*Tfaily et al.*, 2015]. Water is a polar solvent with a selection bias for carbohydrates with high O/C ratios, amino-sugars, and other labile polar compounds [*Malak M Tfaily et al.*, 2015]; and, as nearshore environments frequently experience

159 wetting, water extractions represent an estimation of readily accessible OC compounds in these
160 environments. Conversely, $CHCl_3$ is selective for non-polar lipids associated with mineral
161 interactions and cellular membranes (i.e., physically-bound OC) [*Malak M Tfaily et al.*, 2015].
162 Because MeOH has a polarity in between that of water and $CHCl_3$, it extracts both water-soluble
163 and bound-OC pools (i.e., a mix of compounds that water and $CHCl_3$ extract), and *Tfaily et al.*
164 [2015] have demonstrated compositional overlap between water-soluble and MeOH extracted
165 OC pools. In this study, we are interested in the differences in OC composition between pure
166 water-soluble and bound-OC pools, and we will focus our discussion on H_2O- and $CHCl_3$-
167 extractions only. We use H_2O- and $CHCl_3$-extracted OC as proxies for readily bioavailable (i.e.,
168 weakly bound) vs. less bioavailable (i.e., mineral- and microbial-bound) pools, respectively.
169 Extracts were prepared by adding 1 ml of solvent to 100 mg bulk sediment and shaking in
170 2 mL capped glass vials for two hours on an Eppendorf Thermomixer. Samples were removed
171 from the shaker and left to stand before spinning down and pulling off the supernatant to stop the
172 extraction. The residual sediment was dried with nitrogen gas to remove any remaining solvent,
173 and then the next solvent was added. The $CHCl_3$ and H_2O extracts were diluted in MeOH to
174 improve ESI efficiency. *Tfaily et al.* [2015] estimated the OC extraction efficiency to be ~15%.
175 *Tfaily et al.* [2015] have previously demonstrated extraction efficiencies as low as 2% to be
176 representative of OC pool composition. We further note that numerous studies have established
177 FT-ICR-MS as a robust method for distinguishing compositional differences among OC pools
178 [*Herzsprung et al.*, 2017; *Kellerman et al.*, 2015; *Rossel et al.*, 2016; *Ward and Cory*, 2015;
179 *Zhang et al.*, 2016].
180 Ultra-high resolution mass spectrometry of the three different extracts from each sample
181 was carried out using a 12 Tesla Bruker SolariX FT-ICR-MS located at the Environmental

Molecular Sciences Laboratory (EMSL) in Richland, WA, USA. As per *Tfaily at al.* [2017], we performed weekly calibration using a tuning solution containing C_2F_3O2, $C_6HF_9N_3O$, $C_{12}HF_{21}N_3O$, $C_{20}H_{18}F_{27}N_3O_8P_3$, and $C_{26}H_{18}F_{39}N_3O_8P_3$ with m/z ranging from 112 to 1333 (Agilent Technologies, Santa Clara, CA USA), and instrument settings were optimized using Suwannee River Fulvic Acid (IHSS). The instrument was flushed between samples using a mixture of water and methanol. Blanks were analyzed at the beginning and the end of the day to monitor for background contaminants.

The extracts were injected directly into the mass spectrometer and the ion accumulation time was optimized for all samples to account for differences in OC concentration. The ion accumulation time ranged between 0.5 and 1s. A standard Bruker electrospray ionization (ESI) source was used to generate negatively charged molecular ions. Samples were introduced to the ESI source equipped with a fused silica tube (30 μm i.d.) through an Agilent 1200 series pump (Agilent Technologies) at a flow rate of 3.0 μL min^{-1}. Experimental conditions were as follows: needle voltage, +4.4 kV; Q1 set to 50 *m*/*z*; and the heated resistively coated glass capillary operated at 180 °C.

2.5. FT-ICR-MS data processing

One hundred forty-four individual scans were averaged for each sample and internally calibrated using an organic matter homologous series separated by 14 Da ($–CH_2$ groups). The mass measurement accuracy was less than 1 ppm for singly charged ions across a broad *m*/*z* range (100-1200 *m*/*z*). The mass resolution was ~ 350K at 339 m/z. Data Analysis software (BrukerDaltonik version 4.2) was used to convert raw spectra to a list of m/z values applying

FTMS peak picker module with a signal-to-noise ratio (S/N) threshold set to 7 and absolute intensity threshold to the default value of 100.

Putative chemical formulae were then assigned using in-house software following the Compound Identification Algorithm (CIA), proposed by *Kujawinski and Behn* [2006], modified by *Minor et al.* [2012], and previously described in *Tfaily et al.* [2017]. Chemical formulae were assigned based on the following criteria: S/N >7, and mass measurement error <1 ppm, taking into consideration the presence of C, H, O, N, S and P and excluding other elements. To ensure consistent formula assignment, we aligned all sample peak lists for the entire dataset to each other in order to facilitate consistent peak assignments and eliminate possible mass shifts that would impact formula assignment. We implemented the following rules to further ensure consistent formula assignment: (1) we consistently picked the formula with the lowest error and with the lowest number of heteroatoms and (2) the assignment of one phosphorus atom requires the presence of at least four oxygen atoms.

2.6. Identification of putative biochemical transformations using FT-ICR-MS

To identify potential biochemical transformations, we followed the procedure detailed by *Breitling et al.* [2006] and employed by *Bailey et al.* [2017]. In essence, the mass difference between m/z peaks extracted from each spectrum with S/N>7 were compared to commonly observed mass differences associated with biochemical transformations. All possible pairwise mass differences were calculated within each extraction type for each sample, and differences (within 1ppm) were matched to a list of 92 common biochemical transformations (e.g., gain or loss of amino groups or sugars, Table S1). For example, a mass difference of 99.07 corresponds to a gain or loss of the amino acid valine, while a difference of 179.06 corresponds to the gain or

loss of a glucose molecule. Pairs of peaks with a mass difference within 1 ppm of our transformation list were considered to be related by the corresponding compound. This approach is feasible with FT-ICR-MS data because the set of peaks in each sample are related by measureable and clearly defined mass differences corresponding to gains and losses of compounds. It has been previously used by *Bailey et al.* [2017] to demonstrate differences in biochemical transformations among soils incubated with different microbial inoculate and among pore size classes in complex soil matrices.

2.7. Identification of putative microbial metabolic pathways using FT-IR-MS

Additionally, a set of putative microbial metabolic pathways in each sample can be identified by locating chemical formulae assigned to m/z's within metabolic pathways defined in the Kyoto Encyclopedia of Genes and Genomes (KEGG, Release, 80.0, http://www.kegg.jp) [*Kanehisa and Goto*, 2000]. Chemical formulae were mapped to KEGG pathways using an in-house software to detect all KEGG pathways containing a giving formula. For example, a peak with a mass of 400.3356 was assigned formula $C_{20}H_{16}O_9$ and mapped to KEGG pathway 'map00254' (Aflatoxin biosynthesis) which contains $C_{20}H_{16}O_9$ as an intermediate. While only a subset of compounds detected by FT-ICR-MS are defined within the KEGG database (i.e., peaks must be assigned a chemical formula and that chemical formula must be present in a KEGG pathway), we found 415 unique peaks that were assigned putative molecular formulae *and* that corresponded to compounds present in KEGG pathways. Additionally, we defined assignments at the pathway level (i.e., by "map" number) instead of using enzyme level classification (i.e., EC number) in order to aggregate compounds found within the same pathways. This was done to facilitate functional interpretation.

Although we acknowledge our results do not represent a comprehensive analysis of all microbial metabolic pathways present in a sample, we assume that KEGG pathways containing more peaks detected by FT-ICR-MS within a sample are more likely to be active than those with fewer mapped peaks. We further reduced possible random matches by assessing correlations with aerobic metabolisms as described in the 'Statistical Methods' section below, and we compare results across samples to yield insight into microbial pathways in each sample beyond that which can be garnered from biochemical transformations. The results are, however, conceptually congruent with those derived from the biochemical transformation analyses described in the preceding sub-section. The KEGG pathway and transformation analyses are independent of each other, yet provided consistent insights and thus together they provide greater confidence in our interpretations.

2.8. Statistical Methods

All statistical analyses were conducted using R software (https://www.r-project.org/). FT-ICR m/z intensities were converted into presence/absence data prior to analysis because differences in m/z intensity are influenced by ionization efficiency as well as relative abundance [*Kujawinski and Behn*, 2006; *Minor et al.*, 2012; *Malak M Tfaily et al.*, 2015; *M.M. Tfaily et al.*, 2017].

To examine differences in OC composition between transects, we used the 'vegan' package to construct a Sorenson dissimilarity matrix for all m/z's identified (i.e., we included peaks with or without assigned formula) within each OC pool (water-soluble or physically-bound). Differences between vegetation states (i.e., V vs. NV) were tested with PERMANOVA (999 permutations, 'vegan') and visualized using Non-metric Multidimensional Scaling (NMDS,

273 'vegan'). One sample (NV, profile 1, depth 30-40cm) was removed due to peak interference
274 during FT-ICR-MS, and three samples (NV, profile 2, depths 00-10cm, 10-20cm, 20-30cm) were
275 excluded, because we were unable to collect sufficient sample mass for all analyses.
276 To reveal transformations associated with aerobic metabolism and to study differences in
277 those transformations across vegetation states, we determined the number of times a given
278 transformation occurred within each OC pool in each sample. Specifically, for each of the 92
279 compounds in our set of biochemical transformations, we counted the number of times in each
280 sample that transformation was observed to yield an estimate of the prevalence or 'abundance' of
281 each transformation in each sample. We correlated these abundance estimates to rates of
282 metabolism using Pearson's product-moment correlation coefficient. Positive relationships were
283 inferred as biochemical transformations possibly associated with biotic OC oxidation. To
284 evaluate how transformations associated with OC oxidation varied across vegetation states we
285 used the abundances of those transformations across all samples to calculate Bray-Curtis
286 dissimilarity. Resulting Bray-Curtis dissimilarities were used to visual multivariate differences
287 among samples using non-metric Multidimensional Scaling (NMDS, 'vegan'), and we
288 statistically evaluated separation between vegetation states with PERMANOVA (999
289 permutations, 'vegan'). We refer to H_2O- and $CHCl_3$-soluble OC pools at V and NV,
290 respectively, as V-W ('vegetated water'), V-B ('vegetated bound'), NV-W ('not vegetated
291 water'), and NV-B ('not vegetated bound') for the remainder of the manuscript.
292 Similar to our analyses of biochemical transformations, we found the number of m/z's
293 that mapped to a given KEGG pathway. We make the assumption that pathways with more m/z's
294 mapped to them have a higher probability of actively contributing to biogeochemical function.
295 To identify which pathways were most likely to contribute to aerobic metabolism, we correlated

the number of m/z's mapped to a given KEGG pathway within each sample to aerobic metabolism. Those pathways with positive correlations were interpreted as contributing to OC oxidation, and the following analysis was conducted only with KEGG pathways that positively correlated with aerobic metabolism. The number of peaks mapping to each KEGG pathway in a sample was normalized by the total number of peaks mapping to any positively correlated KEGG pathway in the sample to yield data as a relative abundance. To reveal groups of pathways co-varying with each other across vegetation states and OC pools, we statistically clustered pathways that positively correlated with aerobic metabolism. Clustering was based on pathway relative abundances in each vegetation state and pool type. Clusters were determined using the 'hclust' algorithm in R with the 'complete linkage' clustering method and visualized using the 'pheatmap' package.

Finally, we examined associations between aerobic metabolism and OC thermodynamics by calculating the Gibbs Free Energy of OC oxidation under standard conditions (ΔG^{o}_{Cox}) from the Nominal Oxidation State of Carbon (NOSC) as per *La Rowe and Van Cappellen* [2011]. NOSC was calculated from the number of electrons transferred in OC oxidation half reactions and is defined by the equation:

(1) $NOSC = -((-Z + 4a + b - 3c - 2d + 5e - 2f)/a) + 4$

, where a, b, c, d, e, and f are, respectively, the numbers of C, H, N, O, P, S atoms in a given organic molecule and Z is net charge of the organic molecule (assumed to be 1). In turn, ΔG^{o}_{Cox} was estimated from NOSC following *La Rowe and Van Cappellen* [2011]:

(2) $\Delta G^{o}_{Cox} = 60.3 - 28.5(NOSC)$

Values of ΔG^{o}_{Cox} are generally positive, indicating that OC oxidation must be coupled to the reduction of a terminal electron acceptor. While ΔG^{o}_{Cox} varies according to the availability of

terminal electron acceptors, our system is primarily oxic, allowing us to infer oxygen as the primary electron acceptor in most reactions and make direct comparisons across samples. Additionally, though the exact calculation of ΔG^{o}_{Cox} necessitates an accurate quantification of all species involved in every chemical reaction in a sample, the use of NOSC as a practical basis for determining ΔG^{o}_{Cox} has been validated [*Arndt et al.*, 2013; *LaRowe and Van Cappellen*, 2011].

Here, we assessed relationships between aerobic metabolism and ΔG^{o}_{Cox} of OC compounds identified in each OC pool (determined by FT-ICR-MS analysis) using linear regressions in each vegetation state, in which aerobic metabolism was the independent variable and average ΔG^{o}_{Cox} of all m/z's with assigned formula was the dependent variable.

3. Results and Discussion

3.1. Shifts in physicochemical, metabolic, and OC character between vegetation states

Differences in vegetation states corresponded to differences in physicochemistry, aerobic metabolism, and OC pool composition. V was characterized by mature trees near the water line and was nutrient-rich relative to NV (Figure S1-3). V displayed comparatively high concentrations of total C and rates of aerobic metabolism (Figure S1-3). In contrast, NV consisted of vegetation-free, cobble-ridden shoreline with sandier soils, low total C, and low aerobic metabolism (Figure S1-3).

Compositional difference in OC pools indicated a possibility for distinct OC oxidation processes between the vegetation states (Figure 1), as preferential oxidation of certain OC compounds in each state would be expected to generate an observable difference in OC pool composition. Further, total organic OC content explained only 38% of aerobic metabolic rates ($R^2 = 0.38$, $P < 0.0001$, Figure S4), leaving open the possibility that OC compositional

differences may be related to differences in aerobic metabolism at each vegetation state. The following sections explore this possibility.

3.2. Associations between C transformations and aerobic metabolism

Given compositional differences in OC between vegetation states and known impacts of C chemistry on metabolic functioning in other systems [*Castle et al.*, 2016; *Graham et al.*, 2016b], we hypothesized that biochemical transformations related to rates of aerobic metabolism would be unique to each vegetation state.

Consistent with this hypothesis, transformation analysis indicated that the biochemical processes associated with OC oxidation were significantly different between the vegetation states. Specifically, OC transformations that increased in abundance with increases in aerobic metabolism were significantly different at each vegetation state (PERMANOVA, H_2O $P = 0.022$ and $CHCl_3$ $P = 0.002$, Figure 3 a-b, Table 2). In comparing differences in transformations occurring within the water-soluble OC pool, we observed higher abundances of amino- and sugar-associated transformations for V-W relative to NV-W. Twenty-six of these transformations were identified as contributing to aerobic metabolism in V-W, while none were identified in NV-W. These V-W transformations were primarily associated with simple C molecules (e.g., glucose, alanine, and lysine, Table 2). Conversely, within the bound-OC pool, 38 transformations were identified as contributing to aerobic metabolism in NV-B, compared to only 11 in V-B. In both cases, these transformations consisted of a greater proportion of complex C molecules (e.g., pyridoxal phosphate, palmitic acid, and glyoxylate, Table 2) than in water-soluble pools.

364 The larger number of transformations associated with aerobic metabolism in V-W vs. V-
365 B, and the larger number in NV-B vs. NV-W, suggests that aerobic metabolism in vegetated and
366 unvegetated areas depend on water-soluble and bound-OC pools, respectively. We note some
367 oxidation of the bound-OC pool under vegetated conditions, but only 11 correlations were
368 observed between V-B transformations and aerobic metabolism suggesting a relatively minor
369 role, especially considering that there were 38 significant correlations for NV-B.
370 These differences suggest that an increased supply of bioavailable compounds in
371 vegetated areas leads to bound-OC being less involved in aerobic metabolism, relative to
372 unvegetated areas where bound-OC appears to be heavily involved in aerobic metabolism. The
373 concept of priming [*Kuzyakov*, 2010] would predict the opposite pattern—a greater supply of
374 bioavailable OC should increase the contributions of less bioavailable OC (here, bound-OC) to
375 aerobic metabolism. Our results run counter to a priming mechanism and indicate that the supply
376 of bioavailable compounds—potentially derived from riparian vegetation—diminishes the
377 contribution of bound-OC to aerobic metabolism and, in turn, protects bound-OC pools. Mineral-
378 stabilized OC therefore has greater potential to remain sequestered along river corridors with
379 spatially and temporally consistent inputs of bioavailable OC, potentially derived from riparian
380 vegetation. The fate of OC that moves across the terrestrial-aquatic continuum may therefore be
381 impacted by land use change [*Foley et al.*, 2005] in ways not currently represented in ESMs.
382
383 *3.3. Associations between microbial metabolic pathways and aerobic metabolism*
384 Because we observed stark differences in the identity of OC transformations that
385 correlated with aerobic metabolism across vegetation states, we hypothesized that the microbial
386 metabolic pathways associated with OC transformations were also dependent on vegetation state.

Indeed, pathways associated with OC oxidation were distinct at V vs. NV, supporting our hypothesis that there were differences in the metabolic processing of OC in the presence or absence of riparian vegetation. Specifically, while the metabolism of plant-derived compounds appeared to be a major driver of aerobic respiration at both vegetation states, metabolism at V mostly involved readily bioavailable plant derivatives in the water-soluble OC pool, and metabolism at NV was associated with plant derivatives in the bound-OC pool (Figure 4).

In V-W, two primary pathways were involved in metabolism of plant compounds, each contained within its own hierarchical cluster (map01110: Biosynthesis of secondary metabolites; map00941: Flavonoid biosynthesis). An additional cluster of plant-associated metabolisms with lower abundance in V-W (Cluster 4) was also positively correlated to aerobic metabolism (Figure 4). Each of these pathways denotes an association between plant-derived compounds and OC oxidation in sediments. Secondary metabolites (map01110) are largely comprised of plant-derived compounds such as flavonoids [*Agati et al.*, 2012], terpenoids [*Tholl*, 2015], and nitrogen-containing alkaloids [*Willaman and Schubert*, 1961], while flavonoids [*Agati et al.*, 2012] are one of those most abundant plant-derived compounds. Associations with aflatoxin [*Trail et al.*, 1995], flavone/flavonol [*Agati et al.*, 2012], and phenylpropanoids [*Hahlbrock and Scheel*, 1989] (Cluster 4) bolster this association between plant-associated metabolic pathways and aerobic metabolism in V-W.

Although correlations between plant-associated KEGG pathways and aerobic metabolism could indicate the persistence of plant secondary metabolites rather than microbial metabolism, our results indicate a central role for vegetation in water-soluble OC oxidation in either case. For example, if KEGG associations were attributable to plant metabolism instead of microbial metabolism, correlations between plant-associated pathways and aerobic metabolism in V-W

would indicate an indirect relationship between plant growth and microbial oxidation of OC, whereby plant byproducts support microbial communities in oxidizing other portions of the OC pool.

In contrast to V-W, NV-W did not display associations between plant-associated metabolic pathways and OC oxidation. All significant correlations in NV-W indicated broad metabolic processes including membrane transport and carbohydrate metabolism that may indicate utilization of other resources (Cluster 3, Figure 4).

Instead, we observed relationships between plant-associated metabolisms and OC oxidation within NV-B. For example, correlations with aerobic metabolism were strongest in Cluster 1, which contained pathways of cutin, suberine, and wax biosynthesis [*King et al.*, 2007; *Raffaele et al.*, 2009; *Shepherd and Wynne Griffiths*, 2006], alpha-linolenic acid metabolism [*Crawford et al.*, 2000; *Creelman and Mulpuri*, 2002], and biosynthesis of secondary metabolites [*Agati et al.*, 2012; *Tholl*, 2015; *Willaman and Schubert*, 1961] (Figure 4). Each of these pathways denotes the synthesis or metabolism of a plant-associated lipid compound. Because no specific metabolisms were correlated to OC oxidation in NV-W, we hypothesize that these lipid-based metabolisms comprise the primary KEGG-identifiable pathways associated with OC oxidation in areas without riparian vegetation. We also observed one cluster of pathways that correlated with metabolism at V-B (Cluster 7) and contained plant-associated metabolic pathways such as linoleic acid metabolism [*Crawford et al.*, 2000; *Creelman and Mulpuri*, 2002] and brassinosteroid biosynthesis [*Bishop*, 2007], indicating some oxidation of lipid plant material in the bound-OC pool under vegetated conditions. We therefore propose that plant-derived lipid compounds serve as a secondary substrate for OC oxidation in shorelines with riparian vegetation, given that most correlations at V were detected in the water-soluble pool.

433

434 *3.4. Thermodynamics of carbon oxidation*

435 Finally, we hypothesized that microbes would preferentially oxidize more
436 thermodynamically favorable compounds at both sites, consistent with common thermodynamic
437 constraints on biogeochemical cycles [*Burgin et al.*, 2011; *Hedin et al.*, 1998; *Helton et al.*,
438 2015]. Because we observed evidence for preferential OC oxidation of the water-soluble OC
439 pool at V and of the bound-OC pool at NV, we further hypothesized that thermodynamic-based
440 preference of OC oxidation would be observable only in the preferred substrate pool within each
441 vegetation state. Consistent with this hypothesis, aerobic metabolism was positively correlated to
442 average ΔG^{o}_{Cox} in V-W (R^2 = 0.22, P = 0.03, Fig 5a) and NV-B (R^2 = 0.54, P = 0.001 Fig 5b),
443 but these variables were not correlated in V-B or NV-W. In both cases, aerobic metabolism
444 corresponded to a depletion of more thermodynamically favorable OC (i.e., OC became less
445 favorable as aerobic metabolism increased), resulting in progressively less favorable
446 thermodynamic conditions.

447 The priming conceptual framework would predict that terrestrial inputs associated with
448 riparian vegetation should condition microbial communities to oxidize less thermodynamically
449 favorable C, such as that found in the bound-OC pool. In such a scenario, inputs of
450 thermodynamically favorable carbon should—by minimizing community-level energy
451 constraints—allow for the rise of microbial physiologies that can oxidize less favorable C
452 [*Kuzyakov*, 2010]. In this case, a significant relationship between thermodynamic favorability
453 and aerobic metabolism in the V-W pool should lead to a similar relationship within the V-B
454 pool. Our results reveal a strong relationship within the V-W pool, but not in the V-B pool,

thereby rejecting an influence of priming. Instead, our results suggest that bound-OC pools are protected by thermodynamically favorable compounds that serve as preferred substrate.

In contrast to our expectation that water-soluble OC associated with riparian vegetation would increase oxidation of bound-OC pools, we observed evidence consistent with inhibition of bound-OC oxidation by thermodynamically favorable water-soluble compounds. Priming has been actively debated in aquatic research [*Bengtsson et al.*, 2014; *Bianchi*, 2011; *Guenet et al.*, 2010], and a number of other studies have been unable to detect a priming effect in sediment and aqueous habitats [*Bengtsson et al.*, 2014; *Catalán et al.*, 2015].

The mechanisms resulting in priming are not well understood, but the phenomenon has been associated with nutrient and energy limitations in soil environments [*Kuzyakov*, 2010]. For instance, under nutrient limitation microorganisms may oxidize chemically-complex OC to garner resources (e.g., nitrogen mining), while shared resources that facilitate OC oxidation (e.g., extracellular enzymes) are more likely to facilitate ecological cheating under energy limiting conditions [*Blagodatskaya and Kuzyakov*, 2008; *Catalán et al.*, 2015; *Guenet et al.*, 2010; *Kuzyakov*, 2010]. Our system is oligotrophic, containing a fraction of the total C content observed in other systems (Figure S1) such that C limitation rather than nutrient limitation might drive OC oxidation dynamics. In such a case, readily bioavailable C inputs would be rapidly oxidized but microbial communities may be well-adapted to rely on alternative energy sources (e.g., NH_4^+, Fe) that may be more available than bound-OC pools.

3.5. Conceptual model for OC oxidation at terrestrial-aquatic interfaces

Based on our work, we propose a conceptual model of OC oxidation along terrestrial-aquatic interfaces in which the oxidation of bound-OC is limited by terrestrial inputs from

riparian vegetation (Fig 6. a-b). Riparian vegetation sustains inputs of water-soluble compounds to nearshore OC pools, resulting in a larger thermodynamically favorable, water-soluble OC pool (Figure 6b). This leads to higher overall C content in nearshore sediments and elevated rates of aerobic respiration relative to areas with less riparian vegetation. However, our data suggest that in the presence of riparian vegetation microbial carbon oxidation primarily uses the water-soluble OC pool with minimal oxidation of bound-OC due to physical and/or thermodynamic protection of this pool. For instance, ΔG^{o}_{Cox} was lower in water-soluble OC pools than in bound-OC, and a large presence of this thermodynamically favorable pool may provide adequate substrate to sustain metabolic functioning, limiting the need to metabolize less thermodynamically favorable OC. Additionally, organomineral interactions can protect bound-OC from extracellular enzyme acitivity [*Hunter et al.*, 2016], inhibiting the bioavailability of OC.

In contrast, non-vegetated riparian zones provide little input into water-soluble OC pools (Fig 6a), and rates of metabolism and C pool sizes are lower in these environments. Carbon oxidation in these non-vegetated zones occurs primarily within the bound-OC pool, albeit more slowly and as product of different biochemical and metabolic pathways than in vegetated environments (e.g., complex C transformations and lipid-based metabolism of plant derivatives). We posit that water-soluble pools in non-vegetated sediments are sufficiently small that investing in enzymes needed to metabolize this OC pool results in a net energy loss. Instead, microbes in unvegetated areas must investment in cellular machinery to access bound-OC, and our results imply that the cellular machinery needed to access bound-OC is distinct from the machinery needed to access water-soluble OC.

Interestingly, aerobic metabolism within both types of sediments is related to a depletion of thermodynamically favorable compounds; however, this occurs in water-soluble OC pools in vegetated zones and bound-OC pools in non-vegetated zones. That is, microorganisms in both environments are constrained to the metabolism of their primary substrate pool but preferentially oxidize more thermodynamically favorable compounds within that pool. This suggests that microorganisms are conditioned to metabolize a subset of compounds within sediment OC, possibly defined by thermodynamic or physical protection mechanisms, but operate under common thermodynamic constraints once adapted to oxidize a certain OC pool.

3.6. Broader Implications

Our results indicate that terrestrial C inputs associated with riparian vegetation protect bound-OC from oxidation, possibly aiding long-term storage of mineral-bound pools along river corridors, and our work is particularly relevant to global patterns of CO_2 emissions in light of changes in land cover and increases in C fluxes across the terrestrial-aquatic interface. The magnitude, distribution, and chemical quality of terrestrial C fluxes into aquatic environments are perturbed by shifts in land cover (e.g., due to agriculture, urbanization, and climate-driven vegetation change) [*Fang et al.*, 2005; *Knapp et al.*, 2008]. These fluxes have been examined primarily for their own propensity to be oxidized along land-to-sea continuums [*Battin et al.*, 2008; *Battin et al.*, 2009; *Regnier et al.*, 2013], but we also suggest a role for these fluxes in stabilizing mineral-bound carbon within nearshore environments. For example, vegetation removal, impervious surfaces, and drainage systems coincident with urbanization alter terrestrial C runoff patterns, both changing their magnitude and creating preferential deposition flow paths [*Fraley et al.*, 2009; *Imberger et al.*, 2011; *Smith and Kaushal*, 2015]. Agricultural drainage

systems also lead to preferential flow paths as well as spatiotemporal variation in the quantity and quality of terrestrial-aquatic fluxes [*Graeber et al.*, 2012; *Larson et al.*, 2014], an effect that strongly influences C cycling given that 40% of the earth's land is cultivated [*Foley et al.*, 2005; *Graeber et al.*, 2012]. We propose that changes in the distribution of these fluxes through space and time may impact OC oxidation both in the C transported along these flow paths and within sediments that are differentially exposed to terrestrial OC.

Furthermore, vegetation distributions in natural ecosystems are predicted to shift in response to altered precipitation regimes. Associated changes in plant phenology, morphology, and establishment will impact the quantity, quality, and distribution of terrestrial material entering aquatic systems [*Knapp et al.*, 2008], and we currently have an incomplete understanding of how these patterns will vary across ecosystems and precipitation patterns [*Fang et al.*, 2005; *Knapp et al.*, 2008]. A mechanistic framework for C oxidation that captures impacts of heterogeneity in vegetation in river corridors will therefore aid in predicting how terrestrial-aquatic interfaces respond to ongoing perturbations. Here, we demonstrate a potential for increases in the intensity of terrestrial C fluxes to lead to larger mineral-bound C pools by physically and thermodynamically protecting these pools; and conversely, a potential for oxidation of mineral-bound C pools in areas with diminished terrestrial C inputs.

Earth System Models depend on mathematical representations of C cycling, and the continued development of these models is tightly coupled to conceptual advances drawn from field-based observations [*Burd et al.*, 2016; *Six et al.*, 2002]. Despite recent progress, these models are still missing key regulatory processes [*Todd-Brown et al.*, 2013; *Wieder et al.*, 2013; *Wieder et al.*, 2015]. To address this knowledge gap, we propose a new conceptual framework of OC dynamics based on analysis of *in situ* observational data that explicitly considers a central

546 challenge in model improvement—biochemical, metabolic, and thermodynamic mechanisms
547 governing OC oxidation along terrestrial-aquatic interfaces. Our results directly contrast those
548 expected within a 'priming' framework, and we advance that water-soluble thermodynamically
549 favorable OC associated with riparian vegetation protects thermodynamically less favorable
550 bound-OC from oxidation. We also demonstrate differences in biochemical and metabolic
551 pathways associated with metabolism of water-soluble and bound-OC pools in the presence or
552 absence of riparian vegetation, furthering a processed-based understanding of terrestrial-aquatic
553 interfaces.

554 Our conceptualization of OC oxidation may also be applicable beyond terrestrial-aquatic
555 interfaces, as many ecosystems experience spatiotemporal variability in the quantity of
556 thermodynamically favorable water-soluble OC. For instance, vegetation senescence generates
557 pulses of bioavailable C into most temperate and tropical ecosystems. Our research provides an
558 opportunity to enhance the mechanistic underpinning of OC oxidation process representations
559 within ESMs—an imperative under heterogeneous landscapes and unknown future land cover
560 distributions—and proposes interactions between OC thermodynamics and mineral-inhibition of
561 OC oxidation as a key future research need.

562

563 **Author Contributions.**

564 EBG was responsible for conceptual development and data analysis and was the primary writer
565 with guidance from JCS and MT. ARC, AEG, CTR, ECR, DWK, and JCS were responsible for
566 experimental design and data collection. MT was responsible for all FT-ICR processing. All
567 authors contributed to manuscript revisions.

568

Acknowledgements.

This research was supported by the US Department of Energy (DOE), Office of Biological and Environmental Research (BER), as part of Subsurface Biogeochemical Research Program's Scientific Focus Area (SFA) at the Pacific Northwest National Laboratory (PNNL). PNNL is operated for DOE by Battelle under contract DE-AC06-76RLO 1830. A portion of the research was performed at Environmental Molecular Science Laboratory User Facility. We thank Nancy Hess for helpful feedback in manuscript revision.

578 **References.**
579
580 Aalto, R., L. Maurice-Bourgoin, T. Dunne, D. R. Montgomery, C. A. Nittrouer, and J.-L. Guyot
581 (2003), Episodic sediment accumulation on Amazonian flood plains influenced by El
582 Nino/Southern Oscillation, *Nature*, *425*(6957), 493-497.
583 Agati, G., E. Azzarello, S. Pollastri, and M. Tattini (2012), Flavonoids as antioxidants in plants:
584 location and functional significance, *Plant Science*, *196*, 67-76.
585 Arndt, S., B. B. Jørgensen, D. E. LaRowe, J. Middelburg, R. Pancost, and P. Regnier (2013),
586 Quantifying the degradation of organic matter in marine sediments: a review and synthesis,
587 *Earth-science reviews*, *123*, 53-86.
588 Arntzen, E. V., D. R. Geist, and P. E. Dresel (2006), Effects of fluctuating river flow on
589 groundwater/surface water mixing in the hyporheic zone of a regulated, large cobble bed river,
590 *River Research and Applications*, *22*(8), 937-946.
591 Bailey, V. L., A. Smith, M. Tfaily, S. J. Fansler, and B. Bond-Lamberty (2017), Differences in
592 soluble organic carbon chemistry in pore waters sampled from different pore size domains, *Soil*
593 *Biology and Biochemistry*, *107*, 133-143.
594 Battin, T. J., L. A. Kaplan, S. Findlay, C. S. Hopkinson, E. Marti, A. I. Packman, J. D. Newbold,
595 and F. Sabater (2008), Biophysical controls on organic carbon fluxes in fluvial networks, *Nature*
596 *Geoscience*, *1*(2), 95-100.
597 Battin, T. J., S. Luyssaert, L. A. Kaplan, A. K. Aufdenkampe, A. Richter, and L. J. Tranvik
598 (2009), The boundless carbon cycle, *Nature Geoscience*, *2*(9), 598-600.
599 Bengtsson, M. M., K. Wagner, N. R. Burns, E. R. Herberg, W. Wanek, L. A. Kaplan, and T. J.
600 Battin (2014), No evidence of aquatic priming effects in hyporheic zone microcosms, *Scientific*
601 *reports*, *4*, 5187.
602 Bianchi, T. S. (2011), The role of terrestrially derived organic carbon in the coastal ocean: A
603 changing paradigm and the priming effect, *Proceedings of the National Academy of Sciences*,
604 *108*(49), 19473-19481.
605 Bishop, G. J. (2007), Refining the plant steroid hormone biosynthesis pathway, *Trends in plant*
606 *science*, *12*(9), 377-380.
607 Blagodatskaya, E., and Y. Kuzyakov (2008), Mechanisms of real and apparent priming effects
608 and their dependence on soil microbial biomass and community structure: critical review,
609 *Biology and Fertility of Soils*, *45*(2), 115-131.
610 Breitling, R., S. Ritchie, D. Goodenowe, M. L. Stewart, and M. P. Barrett (2006), Ab initio
611 prediction of metabolic networks using Fourier transform mass spectrometry data,
612 *Metabolomics*, *2*(3), 155-164.
613 Burd, A. B., S. Frey, A. Cabre, T. Ito, N. M. Levine, C. Lønborg, M. Long, M. Mauritz, R. Q.
614 Thomas, and B. M. Stephens (2016), Terrestrial and marine perspectives on modeling organic
615 matter degradation pathways, *Global change biology*, *22*(1), 121-136.
616 Burgin, A. J., W. H. Yang, S. K. Hamilton, and W. L. Silver (2011), Beyond carbon and
617 nitrogen: how the microbial energy economy couples elemental cycles in diverse ecosystems,
618 *Frontiers in Ecology and the Environment*, *9*(1), 44-52.
619 Castle, S. C., D. R. Nemergut, A. S. Grandy, J. W. Leff, E. B. Graham, E. Hood, S. K. Schmidt,
620 K. Wickings, and C. C. Cleveland (2016), Biogeochemical drivers of microbial community
621 convergence across actively retreating glaciers, *Soil Biology and Biochemistry*, *101*, 74-84.

622 Catalán, N., A. M. Kellerman, H. Peter, F. Carmona, and L. J. Tranvik (2015), Absence of a
623 priming effect on dissolved organic carbon degradation in lake water, *Limnology and*
624 *Oceanography*, *60*(1), 159-168.
625 Cotrufo, M. F., M. D. Wallenstein, C. M. Boot, K. Denef, and E. Paul (2013), The Microbial
626 Efficiency‐Matrix Stabilization (MEMS) framework integrates plant litter decomposition with
627 soil organic matter stabilization: do labile plant inputs form stable soil organic matter?, *Global*
628 *Change Biology*, *19*(4), 988-995.
629 Crawford, M., C. Galli, F. Visioli, S. Renaud, A. P. Simopoulos, and A. A. Spector (2000), Role
630 of plant-derived omega–3 fatty acids in human nutrition, *Annals of Nutrition and Metabolism*,
631 *44*(5-6), 263-265.
632 Creelman, R. A., and R. Mulpuri (2002), The oxylipin pathway in Arabidopsis, *The Arabidopsis*
633 *Book*, e0012.
634 Dorado-García, I., J. Syväranta, S. P. Devlin, J. M. Medina-Sánchez, and R. I. Jones (2016),
635 Experimental assessment of a possible microbial priming effect in a humic boreal lake, *Aquatic*
636 *Sciences*, *78*(1), 191-202.
637 Ebel, W. J., C. D. Becker, J. W. Mullan, and H. L. Raymond (1989), The Columbia River--
638 toward a holistic understanding, *Canadian special publication of fisheries and aquatic*
639 *sciences/Publication speciale canadienne des sciences halieutiques et aquatiques. 1989.*
640 Fang, J., S. Piao, L. Zhou, J. He, F. Wei, R. B. Myneni, C. J. Tucker, and K. Tan (2005),
641 Precipitation patterns alter growth of temperate vegetation, *Geophysical research letters*, *32*(21).
642 Foley, J. A., R. DeFries, G. P. Asner, C. Barford, G. Bonan, S. R. Carpenter, F. S. Chapin, M. T.
643 Coe, G. C. Daily, and H. K. Gibbs (2005), Global consequences of land use, *science*, *309*(5734),
644 570-574.
645 Fraley, L. M., A. J. Miller, and C. Welty (2009), Contribution of In‐Channel Processes to
646 Sediment Yield of an Urbanizing Watershed1, *JAWRA Journal of the American Water Resources*
647 *Association*, *45*(3), 748-766.
648 Graeber, D., J. Gelbrecht, M. T. Pusch, C. Anlanger, and D. von Schiller (2012), Agriculture has
649 changed the amount and composition of dissolved organic matter in Central European headwater
650 streams, *Science of the Total Environment*, *438*, 435-446.
651 Graham, E. B., A. R. Crump, C. T. Resch, S. Fansler, E. Arntzen, D. W. Kennedy, J. K.
652 Fredrickson, and J. C. Stegen (2016a), Coupling spatiotemporal community assembly processes
653 to changes in microbial metabolism, *Frontiers in Microbiology*, *7*, 1949.
654 Graham, E. B., A. R. Crump, C. T. Resch, S. Fansler, E. Arntzen, D. W. Kennedy, J. K.
655 Fredrickson, and J. C. Stegen (2017), Deterministic influences exceed dispersal effects on
656 hydrologically‐connected microbiomes, *Environmental Microbiology*, *19*(4), 1552-1567.
657 Graham, E. B., J. E. Knelman, R. S. Gabor, S. Schooler, D. M. McKnight, and D. Nemergut
658 (2016b), Dissolved organic matter and inorganic mercury loadings favor novel methylators and
659 fermentation metabolisms in oligotrophic sediments, *bioRxiv*, 072017.
660 Guenet, B., M. Danger, L. Abbadie, and G. Lacroix (2010), Priming effect: bridging the gap
661 between terrestrial and aquatic ecology, *Ecology*, *91*(10), 2850-2861.
662 Haggerty, R., E. Martí, A. Argerich, D. Von Schiller, and N. B. Grimm (2009), Resazurin as a
663 “smart” tracer for quantifying metabolically active transient storage in stream ecosystems,
664 *Journal of Geophysical Research: Biogeosciences*, *114*(G3).
665 Hahlbrock, K., and D. Scheel (1989), Physiology and molecular biology of phenylpropanoid
666 metabolism, *Annual review of plant biology*, *40*(1), 347-369.

667 Hedges, J., and J. Oades (1997), Comparative organic geochemistries of soils and marine
668 sediments, *Organic geochemistry*, *27*(7), 319-361.
669 Hedges, J. I., G. Eglinton, P. G. Hatcher, D. L. Kirchman, C. Arnosti, S. Derenne, R. P.
670 Evershed, I. Kögel-Knabner, J. De Leeuw, and R. Littke (2000), The molecularly-
671 uncharacterized component of nonliving organic matter in natural environments, *Organic*
672 *Geochemistry*, *31*(10), 945-958.
673 Hedges, J. I., and R. G. Keil (1995), Sedimentary organic matter preservation: an assessment and
674 speculative synthesis, *Marine chemistry*, *49*(2-3), 81-115.
675 Hedin, L. O., J. C. von Fischer, N. E. Ostrom, B. P. Kennedy, M. G. Brown, and G. P. Robertson
676 (1998), Thermodynamic constraints on nitrogentransformations and other
677 biogeochemicalprocesses at soil–stream interfaces, *Ecology*, *79*(2), 684-703.
678 Helton, A. M., M. Ardón, and E. S. Bernhardt (2015), Thermodynamic constraints on the utility
679 of ecological stoichiometry for explaining global biogeochemical patterns, *Ecology letters*,
680 *18*(10), 1049-1056.
681 Herzsprung, P., K. Osterloh, W. von Tümpling, M. Harir, N. Hertkorn, P. Schmitt-Kopplin, R.
682 Meissner, S. Bernsdorf, and K. Friese (2017), Differences in DOM of rewetted and natural
683 peatlands–Results from high-field FT-ICR-MS and bulk optical parameters, *Science of The Total*
684 *Environment*, *586*, 770-781.
685 Hunter, W. R., R. Niederdorfer, A. Gernand, B. Veuger, J. Prommer, M. Mooshammer, W.
686 Wanek, and T. J. Battin (2016), Metabolism of mineral‐sorbed organic matter and microbial
687 lifestyles in fluvial ecosystems, *Geophysical Research Letters*.
688 Imberger, S. J., R. M. Thompson, and M. R. Grace (2011), Urban catchment hydrology
689 overwhelms reach scale effects of riparian vegetation on organic matter dynamics, *Freshwater*
690 *Biology*, *56*(7), 1370-1389.
691 Kanehisa, M., and S. Goto (2000), KEGG: kyoto encyclopedia of genes and genomes, *Nucleic*
692 *acids research*, *28*(1), 27-30.
693 Kellerman, A. M., D. N. Kothawala, T. Dittmar, and L. J. Tranvik (2015), Persistence of
694 dissolved organic matter in lakes related to its molecular characteristics, *Nature Geoscience*,
695 *8*(6), 454-457.
696 Kim, S., R. W. Kramer, and P. G. Hatcher (2003), Graphical method for analysis of ultrahigh-
697 resolution broadband mass spectra of natural organic matter, the van Krevelen diagram,
698 *Analytical Chemistry*, *75*(20), 5336-5344.
699 King, A., J.-W. Nam, J. Han, J. Hilliard, and J. G. Jaworski (2007), Cuticular wax biosynthesis
700 in petunia petals: cloning and characterization of an alcohol-acyltransferase that synthesizes
701 wax-esters, *Planta*, *226*(2), 381-394.
702 Knapp, A. K., C. Beier, D. D. Briske, A. T. Classen, Y. Luo, M. Reichstein, M. D. Smith, S. D.
703 Smith, J. E. Bell, and P. A. Fay (2008), Consequences of more extreme precipitation regimes for
704 terrestrial ecosystems, *Bioscience*, *58*(9), 811-821.
705 Koch, B. P., M. Witt, R. Engbrodt, T. Dittmar, and G. Kattner (2005), Molecular formulae of
706 marine and terrigenous dissolved organic matter detected by electrospray ionization Fourier
707 transform ion cyclotron resonance mass spectrometry, *Geochimica et Cosmochimica Acta*,
708 *69*(13), 3299-3308.
709 KoÈgel-Knabner, I. (2002), The macromolecular organic composition of plant and microbial
710 residues as inputs to soil organic matter, *Soil Biology and Biochemistry*, *34*(2), 139-162.
711 Kögel-Knabner, I. (2000), Analytical approaches for characterizing soil organic matter, *Organic*
712 *Geochemistry*, *31*(7), 609-625.

Kujawinski, E. B., and M. D. Behn (2006), Automated analysis of electrospray ionization Fourier transform ion cyclotron resonance mass spectra of natural organic matter, *Analytical Chemistry*, *78*(13), 4363-4373.

Kuzyakov, Y. (2010), Priming effects: interactions between living and dead organic matter, *Soil Biology and Biochemistry*, *42*(9), 1363-1371.

LaRowe, D. E., and P. Van Cappellen (2011), Degradation of natural organic matter: a thermodynamic analysis, *Geochimica et Cosmochimica Acta*, *75*(8), 2030-2042.

Larson, J. H., P. C. Frost, M. A. Xenopoulos, C. J. Williams, A. M. Morales-Williams, J. M. Vallazza, J. C. Nelson, and W. B. Richardson (2014), Relationships between land cover and dissolved organic matter change along the river to lake transition, *Ecosystems*, *17*(8), 1413-1425.

Lehmann, J., and M. Kleber (2015), The contentious nature of soil organic matter, *Nature*, *528*(7580), 60-68.

Lin, X., J. McKinley, C. T. Resch, R. Kaluzny, C. L. Lauber, J. Fredrickson, R. Knight, and A. Konopka (2012), Spatial and temporal dynamics of the microbial community in the Hanford unconfined aquifer, *The ISME Journal*, *6*(9), 1665-1676.

Lotspeich, F. B., and B. H. Reid (1980), Tri-tube freeze-core procedure for sampling stream gravels, *The Progressive Fish-Culturist*, *42*(2), 96-99.

Mason, H., J. Begg, R. S. Maxwell, A. B. Kersting, and M. Zavarin (2016), A novel solid-state NMR method for the investigation of trivalent lanthanide sorption on amorphous silica at low surface loadings, *Environmental Science: Processes & Impacts*.

Minor, E. C., C. J. Steinbring, K. Longnecker, and E. B. Kujawinski (2012), Characterization of dissolved organic matter in Lake Superior and its watershed using ultrahigh resolution mass spectrometry, *Organic Geochemistry*, *43*, 1-11.

Moser, D. P., J. K. Fredrickson, D. R. Geist, E. V. Arntzen, A. D. Peacock, S.-M. W. Li, T. Spadoni, and J. P. McKinley (2003), Biogeochemical processes and microbial characteristics across groundwater-surface water boundaries of the Hanford Reach of the Columbia River, *Environmental Science & Technology*, *37*(22), 5127-5134.

Peterson, R. E., and M. P. Connelly (2004), Water movement in the zone of interaction between groundwater and the Columbia River, Hanford site, Washington, *Journal of Hydraulic Research*, *42*(S1), 53-58.

Raffaele, S., A. Leger, and D. Roby (2009), Very long chain fatty acid and lipid signaling in the response of plants to pathogens, *Plant signaling & behavior*, *4*(2), 94-99.

Regnier, P., P. Friedlingstein, P. Ciais, F. T. Mackenzie, N. Gruber, I. A. Janssens, G. G. Laruelle, R. Lauerwald, S. Luyssaert, and A. J. Andersson (2013), Anthropogenic perturbation of the carbon fluxes from land to ocean, *Nature geoscience*, *6*(8), 597-607.

Rood, K., and M. Church (1994), Modified freeze-core technique for sampling the permanently wetted streambed, *North American Journal of Fisheries Management*, *14*(4), 852-861.

Rossel, P. E., C. Bienhold, A. Boetius, and T. Dittmar (2016), Dissolved organic matter in pore water of Arctic Ocean sediments: Environmental influence on molecular composition, *Organic Geochemistry*, *97*, 41-52.

Rothman, D. H., and D. C. Forney (2007), Physical model for the decay and preservation of marine organic carbon, *Science*, *316*(5829), 1325-1328.

Schmidt, M. W., M. S. Torn, S. Abiven, T. Dittmar, G. Guggenberger, I. A. Janssens, M. Kleber, I. Kögel-Knabner, J. Lehmann, and D. A. Manning (2011), Persistence of soil organic matter as an ecosystem property, *Nature*, *478*(7367), 49-56.

Shepherd, T., and D. Wynne Griffiths (2006), The effects of stress on plant cuticular waxes, *New Phytologist*, *171*(3), 469-499.

Six, J., P. Callewaert, S. Lenders, S. De Gryze, S. Morris, E. Gregorich, E. Paul, and K. Paustian (2002), Measuring and understanding carbon storage in afforested soils by physical fractionation, *Soil science society of America journal*, *66*(6), 1981-1987.

Slater, L. D., D. Ntarlagiannis, F. D. Day‐Lewis, K. Mwakanyamale, R. J. Versteeg, A. Ward, C. Strickland, C. D. Johnson, and J. W. Lane (2010), Use of electrical imaging and distributed temperature sensing methods to characterize surface water–groundwater exchange regulating uranium transport at the Hanford 300 Area, Washington, *Water Resources Research*, *46*(10).

Smith, R. M., and S. S. Kaushal (2015), Carbon cycle of an urban watershed: exports, sources, and metabolism, *Biogeochemistry*, *126*(1-2), 173-195.

Stegen, J. C., J. K. Fredrickson, M. J. Wilkins, A. E. Konopka, W. C. Nelson, E. V. Arntzen, W. B. Chrisler, R. K. Chu, R. E. Danczak, and S. J. Fansler (2016), Groundwater-surface water mixing shifts ecological assembly processes and stimulates organic carbon turnover, *Nature Communications*, *7*.

Stegen, J. C., X. Lin, A. E. Konopka, and J. K. Fredrickson (2012), Stochastic and deterministic assembly processes in subsurface microbial communities, *The ISME Journal*, *6*(9), 1653-1664.

Tfaily, M. M., R. K. Chu, N. Tolić, K. M. Roscioli, C. R. Anderton, L. Pasa-Tolić, E. W. Robinson, and N. J. Hess (2015), Advanced solvent based methods for molecular characterization of soil organic matter by high-resolution mass spectrometry, *Analytical chemistry*, *87*(10), 5206-5215.

Tfaily, M. M., D. C. Podgorski, J. E. Corbett, J. P. Chanton, and W. T. Cooper (2011), Influence of acidification on the optical properties and molecular composition of dissolved organic matter, *Analytica chimica acta*, *706*(2), 261-267.

Tfaily, M. M., P. Reardon, R. K. Chu, N. Tolić, L. Pasa-Tolić, E. W. Robinson, and N. J. Hess (2017), Sequential extraction protocol for organic matter from soils and sediments using high resolution mass spectrometry and proton NMR, *Analytica Chimica Acta*.

Tholl, D. (2015), Biosynthesis and biological functions of terpenoids in plants, in *Biotechnology of Isoprenoids*, edited, pp. 63-106, Springer.

Todd-Brown, K., J. Randerson, W. Post, F. Hoffman, C. Tarnocai, E. Schuur, and S. Allison (2013), Causes of variation in soil carbon simulations from CMIP5 Earth system models and comparison with observations, *Biogeosciences*, *10*(3).

Trail, F., N. Mahanti, and J. Linz (1995), Molecular biology of aflatoxin biosynthesis, *Microbiology*, *141*(4), 755-765.

Tremblay, L. B., T. Dittmar, A. G. Marshall, W. J. Cooper, and W. T. Cooper (2007), Molecular characterization of dissolved organic matter in a North Brazilian mangrove porewater and mangrove-fringed estuaries by ultrahigh resolution Fourier transform-ion cyclotron resonance mass spectrometry and excitation/emission spectroscopy, *Marine chemistry*, *105*(1), 15-29.

Ward, C. P., and R. M. Cory (2015), Chemical composition of dissolved organic matter draining permafrost soils, *Geochimica et Cosmochimica Acta*, *167*, 63-79.

Wieder, W. R., G. B. Bonan, and S. D. Allison (2013), Global soil carbon projections are improved by modelling microbial processes, *Nature Climate Change*, *3*(10), 909-912.

Wieder, W. R., C. C. Cleveland, W. K. Smith, and K. Todd-Brown (2015), Future productivity and carbon storage limited by terrestrial nutrient availability, *Nature Geoscience*, *8*(6), 441-444.

Willaman, J. J., and B. G. Schubert (1961), *Alkaloid-bearing plants and their contained alkaloids*, Agricultural Research Service, US Department of Agriculture.

804 Zachara, J. M., P. E. Long, J. Bargar, J. A. Davis, P. Fox, J. K. Fredrickson, M. D. Freshley, A.
805 E. Konopka, C. Liu, and J. P. McKinley (2013), Persistence of uranium groundwater plumes:
806 Contrasting mechanisms at two DOE sites in the groundwater–river interaction zone, *Journal of*
807 *Contaminant Hydrology*, *147*, 45-72.
808 Zhang, L., S. Wang, Y. Xu, Q. Shi, H. Zhao, B. Jiang, and J. Yang (2016), Molecular
809 characterization of lake sediment WEON by Fourier transform ion cyclotron resonance mass
810 spectrometry and its environmental implications, *Water Research*, *106*, 196-203.
811
812

813 **Figures and Tables.**

Figure 1

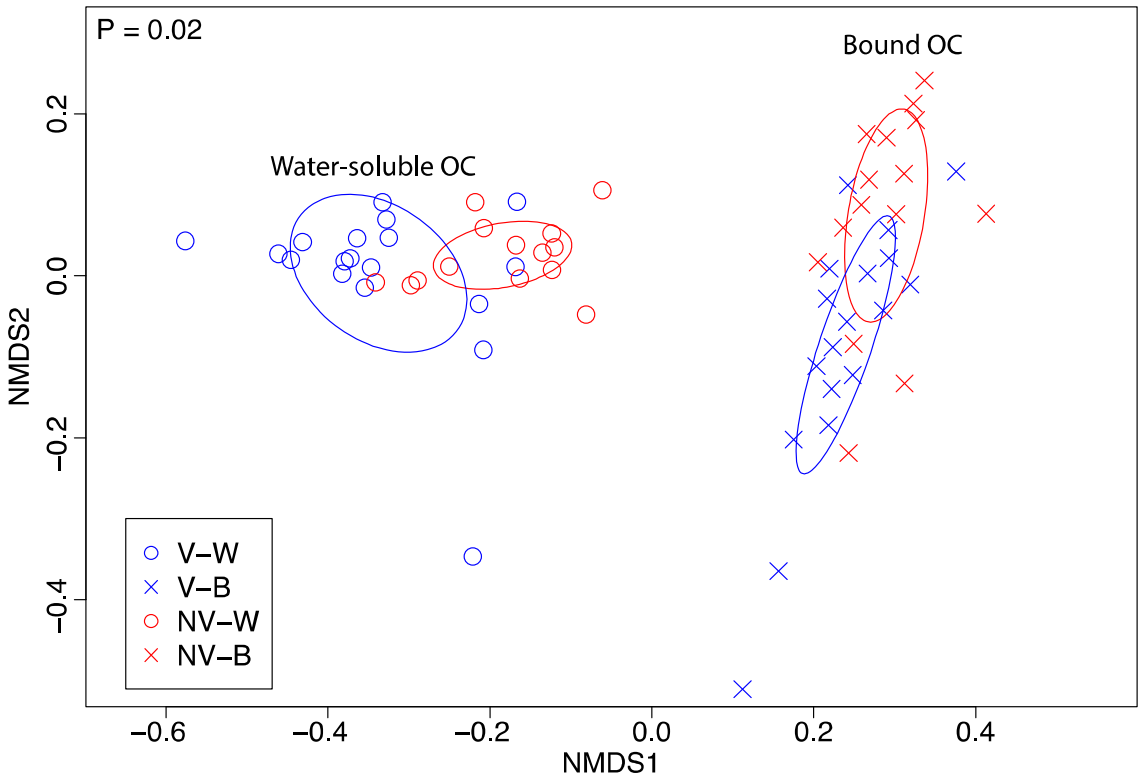

814

815 **Figure 1. NMDS visualization of dissimilarity in OC pool composition.** Water-soluble and
816 bound-OC pools are represented by open circles and x's, respectively. Samples associated with
817 riparian vegetation are blue, and those in areas without vegetation are red. The P-value reflects
818 differences among all groups, as assessed by PERMANOVA. Ellipses represent the standard
819 deviation of the average axis scores for each group, generated using the 'ordiellipse' function in
820 the 'vegan' package. Within each extraction, the composition of OC pools was significantly
821 different across vegetation states (both P = 0.001).

822

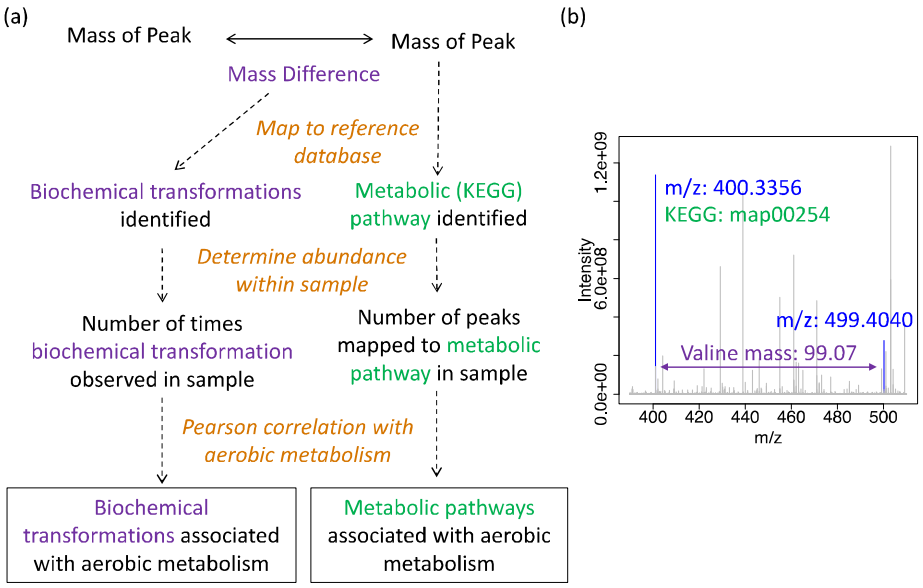

Figure 2. Methodology for inferring biochemical transformations and metabolic pathways. Panel (a) depicts our workflow for analyzing biochemical transformations and metabolic pathways. Biochemical OC transformations (purple) were identified by mapping mass differences in pairwise m/z peak comparisons to a set of 92 known masses transferred in common biochemical transformations (e.g., glucose, amines). Metabolic pathways (green) were identified by mapping all chemical formula assigned to m/z peaks to the KEGG database. Within each sample, the abundance of each biochemical transformation and the number of peaks mapping to each metabolic pathway were then correlated to aerobic metabolism to garner insights into OC oxidation processes. Panel (b) displays an example portion of our FT-ICR-MS spectra overlain with peak assignments (blue), a biochemical transformation (mass difference between peaks, denoted in purple), and a metabolic pathway (associated with the left-hand peak, denoted in green).

Figure 3

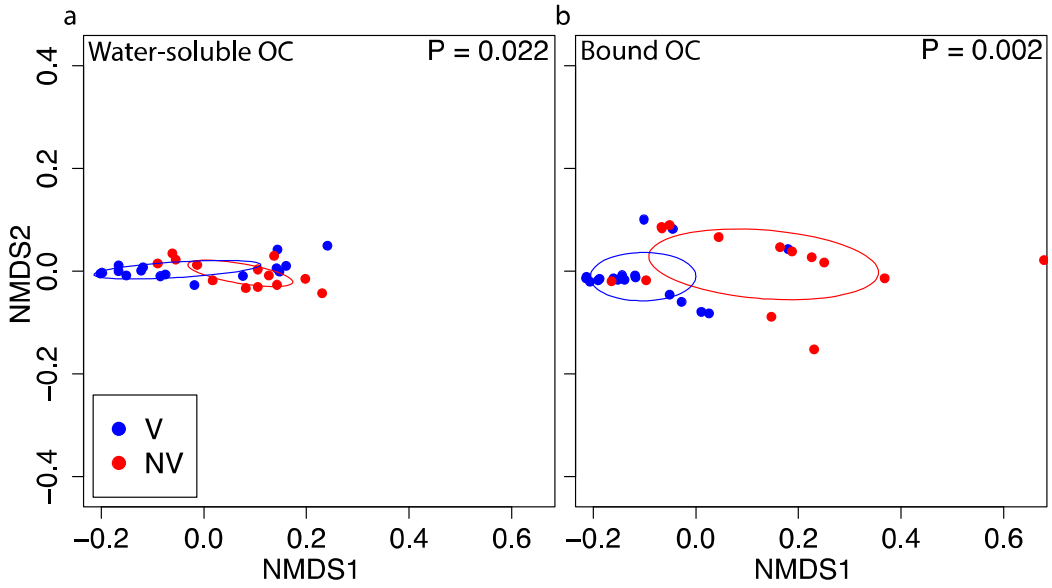

837

838 **Figure 3. NMDS visualization of biochemical transformation partitioning among vegetation**

839 **states.** Biochemical transformations that were correlated to aerobic metabolism were

840 significantly different among vegetation states in both the (a) water-soluble and (b) bound-OC

841 pools. V and NV are denoted in blue and red, respectively, and significance values are derived

842 from PERMANOVA. Ellipses represent the standard deviation of the average axis scores for

843 each group, generated using the 'ordiellipse' function in the 'vegan' package.

Figure 4

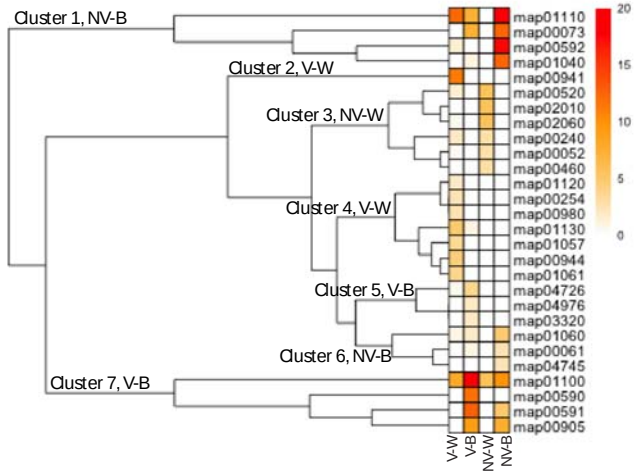

	Pathway	Pathway Description
	map01110	Biosynthesis of secondary metabolites
Cluster 1	map00073	Cutin, suberine and wax biosynthesis
NV-B	map00592	alpha-Linolenic acid metabolism
	map01040	Biosynthesis of unsaturated fatty acids
Cluster 2	map00941	Flavonoid biosynthesis
V-W		
	map00520	Amino sugar and nucleotide sugar metabolism
	map02010	ABC transporters
Cluster 3	map02060	Phosphotransferase system (PTS)
NV-W	map00240	Pyrimidine metabolism
	map00052	Galactose metabolism
	map00460	Cyanoamino acid metabolism
	map01120	Microbial metabolism in diverse environments
	map00254	Aflatoxin biosynthesis
Cluster 4	map00980	Metabolism of xenobiotics by cytochrome P450
V-W	map01130	Biosynthesis of antibiotics
	map01057	Biosynthesis of type II polyketide products
	map00944	Flavone and flavonol biosynthesis
	map01061	Biosynthesis of phenylpropanoids
	map04726	Serotonergic synapse
Cluster 5	map04976	Bile secretion
V-B	map03320	PPAR signaling pathway
	map01060	Biosynthesis of plant secondary metabolites
Cluster 6	map00061	Fatty acid biosynthesis
NV-B	map04745	Phototransduction - fly
	map01100	Metabolic pathways
Cluster 7	map00590	Arachidonic acid metabolism
V-B	map00591	Linoleic acid metabolism
	map00905	Brassinosteroid biosynthesis

844

845 **Figure 4. KEGG pathways associated with aerobic metabolism.** A hierarchical clustering
846 heatmap shows KEGG pathways positively associated with aerobic metabolism. Colors move
847 from white to red from a scale of 0% to 20%, showing percent relative abundance of each
848 pathway in each group. Pathways are described and divided by cluster and listed in the legend.
849 V-W, V-B, NV-W, and NV-B are placed on branches that yield clusters with which they are
850 predominantly associated.

Figure 5

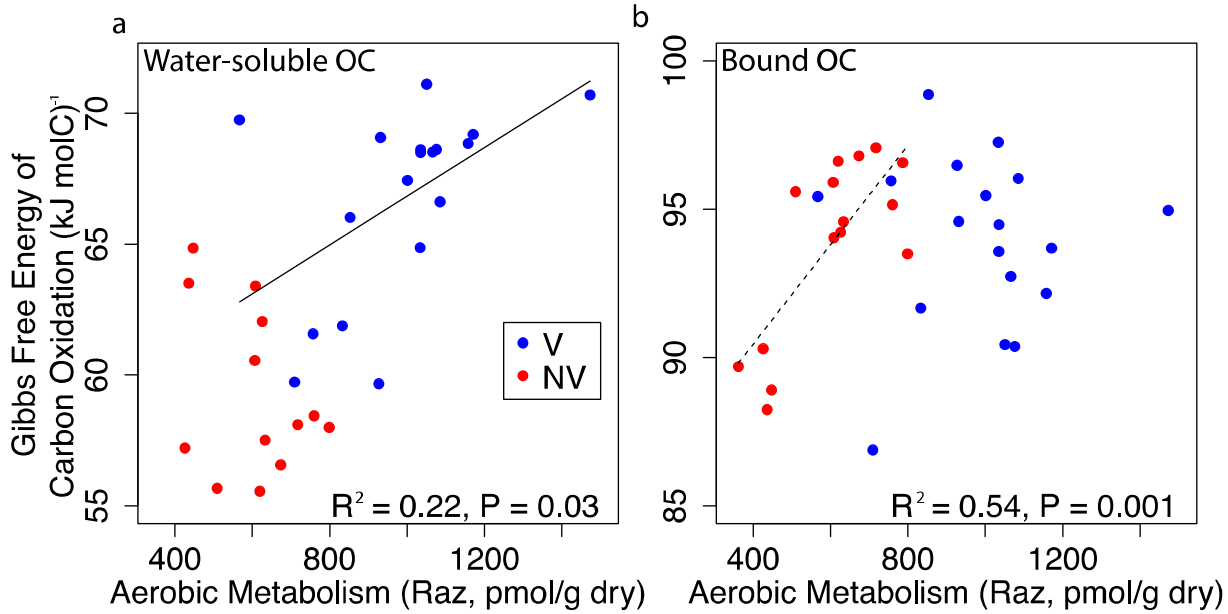

Figure 5. Correlations between Gibbs free energy of carbon oxidation (ΔG^{o}_{Cox}) and aerobic metabolism. (a) and (b) display linear regressions relating ΔG^{o}_{Cox} to aerobic metabolism in water-soluble and bound-OC pools, respectively. Aerobic metabolism is expressed as pmoles of resazurin reduced to resorufin per gram dry weight over a 48hr incubation period (Raz, see Supplemental Information). V and NV are denoted in blue and red. Solid lines show significant relationship at V; dashed lines show significant relationship at NV.

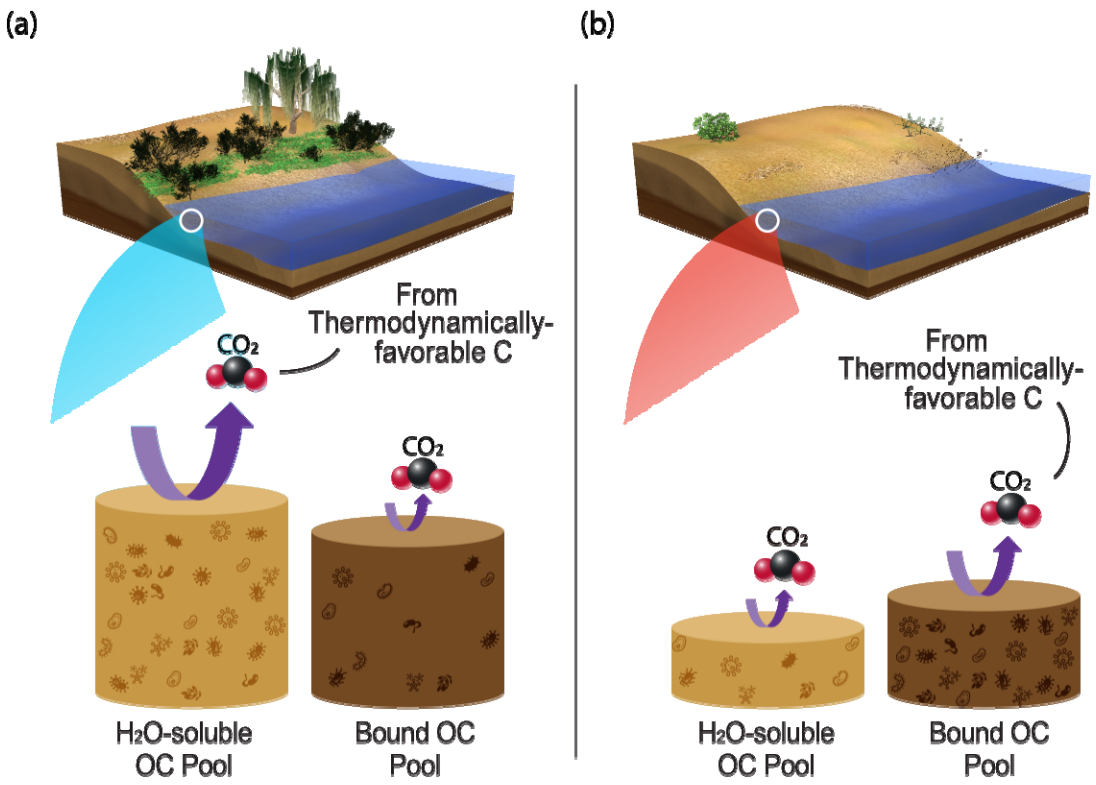

858

859 **Figure 6. Conceptualization of relationship between riparian vegetation and OC oxidation.**

860 We propose a conceptualization of OC oxidation at terrestrial-aquatic interfaces whereby (a)

861 more riparian vegetation results in greater terrestrial C deposition and larger water-soluble and

862 bound-OC pools. However, water-soluble OC is preferentially oxidized, which protects the

863 bound-OC pool. Conversely, (b) areas deplete in riparian vegetation experience lower inputs to

864 water-soluble OC pools and show lower rates of OC oxidation. This results in smaller OC pools

865 (water-soluble and bound) and microbial adaptation for oxidation of the bound-OC pool. In both

866 cases, the most thermodynamically favorable portions of the OC pool being metabolized are

867 preferentially oxidized. Height of the cylinders denotes pool sizes, and arrow thickness denotes

868 flux magnitude.

869

870

871 **Table 1. Acronyms and abbreviations used in this paper.**

Abbreviation/Acronym	Description
V	Transect with dense riparian vegetation (i.e., 'vegetated')
NV	Transect with sparse riparian vegetation (i.e., 'not vegetated')
V-W	Transect V, water extraction (water-soluble OC)
V-B	Transect V, chloroform extraction (bound-OC)
NV-W	Transect NV, water extraction (water-soluble OC)
NV-B	Transect NV, chloroform extraction (bound-OC)
H_2O	Water
$CHCl_3$	Chloroform
C	Carbon
OC	Organic carbon
FT-ICR-MS	Fourier transform ion cyclotron resonance mass spectrometry
KEGG	Kyoto Encyclopedia of Genes and Genomes
ΔG^{o}_{Cox}	Gibbs free energy of C oxidation

872

873 **Table 2. Biochemical transformations correlated with aerobic metabolism in each OC pool**

874 **and vegetation state.**

	Pearson's r
V-W	
biotinyl_(-H)_C10H15N2O3S	0.74
uridine_5_diphosphate_(-H2O)_C9H12N2O11P2	0.67
cytosine_(-H)_C4H4N3O	0.65
uridine_5_monophosphate_(-H2O)_C9H11N2O8P	0.65
guanine_(-H)_C5H4N5O	0.61
guanosine_(-H2O)_C10H11N5O4	0.59
adenine_(-H)_C5H4N5	0.59
glutathione_(-H2O)_C10H15N3O5S	0.57
uracil_(-H)_C4H3N2O2	0.56
glucose_C6H12O6	0.53
C6H10O6	0.53
Aspartic_Acid_C4H5NO3	0.52
GlucuronicAcid(-H2O)	0.52
Lysine_C6H12N2O	0.51
D-Ribose(-H2O)(ribosylation)	0.50
secondaryamine	0.50
Alanine_C3H5NO	0.50
C6H10O5	0.49
monosaccharide(-H2O)	0.49
Threonine_C4H7NO2	0.49
Glutamic_Acid_C5H7NO3	0.48
pentose_C5H8O4	0.47
acetotacetate_(-H2O)_C4H4O2	0.47
Glutamine_C5H8N2O2	0.47
pyridoxal_phosphate_(-H2O)_C8H8NO5P	0.47
V-B	
isoprene_addition_(-H)_C5H7	0.61
phosphate	0.56
primaryamine	0.55
GlucuronicAcid(-H2O)	0.53
glyoxylate_(-H2O)_C2O2	0.53
malonyl_group_(-H2O)_C3H2O3	0.52
D-Ribose(-H2O)(ribosylation)	0.49
pyrophosphate	0.49
acetotacetate_(-H2O)_C4H4O2	0.49
hydrogenation_dehydrogenation_H2	0.47

875

876

NV-W	
NONE	NA
NV-B	
Adenosine_5_monophosphate_(-H2O)_C10H12N5O6P	0.92
adenylate_(-H2O)_C10H12N5O6P	0.92
pyridoxal_phosphate_(-H2O)_C8H8NO5P	0.73
acetylation_(-H2O)_C2H2O	0.70
ketol group (-H2O)	0.70
Isoleucine_C6H11NO	0.69
Leucine_C6H11NO	0.69
ethyl addition_(-H2O)_C2H4	0.69
Threonine_C4H7NO2	0.69
Valine_C5H9NO	0.68
Carboxylation_CO2	0.68
Glycine_C2H3NO	0.67
Formic Acid_(-H2O)_CO	0.67
Serine_C3H5NO2	0.67
hydroxylation_(-H)_O	0.67
palmitoylation_(-H2O)_C16H30O	0.67
pentose_C5H8O4	0.66
secondary amine	0.66
condensation/dehydration_H2O	0.66
C2H2_C2H2	0.66
erythose (-H2O)	0.66
CH4_O	0.65
methanol (-H2O)	0.65
glyoxylate_(-H2O)_C2O2	0.65
NH_CH2	0.64
Alanine_C3H5NO	0.63
acetotacetate_(-H2O)_C4H4O2	0.63
Proline_C5H7NO	0.62
hydrogenation_dehydrogenation_H2	0.61
Histidine_C6H7N3O	0.60
malonyl_group_(-H2O)_C3H2O3	0.59
Cysteine_C3H5NOS	0.58
glcnac_C8H13N1O5	0.57
Methionine_C5H9NOS	0.57
Arginine_C6H12N4O	0.56
Aspartic_Acid_C4H5NO3	0.56

D-Ribose (-H2O) (ribosylation)	0.55